INVESTIGATION OF PASSIVE MAGNETIC BEARING WITH HALBACH-ARRAY

Arkadiusz MYSTKOWSKI[*], Leszek AMBROZIAK[*]

[*]Bialystok University of Technology, Faculty of Mechanical Engineering
Wiejska 45 C, 15-351 Bialystok

a.mystkowski@pb.edu.pl, leszek.ambroziak@gmail.com

Abstract: The paper has describes the complete design and investigation processes of permanent magnetic bearing. The passive magnetic bearing (PMB) rotor suspension rig employing no active control components was calculated, designed, constructed and tested. In order to increase the radial passive magnetic bearing stiffness, the Halbach-array configuration was used. The main purpose of the work was developing the nonlinear model of the PMB. Therefore, the magnetic flux circuit of the PMB was analytically calculated by using the Ohm and Kirchhoff methods. The nonlinear effects of the discrete 3D model of the PMB was analyzed using Finite Element Method (FEM). Finally, the very well matched experimental and analytical static characteristics of the passive magnetic suspension were carried out.

1. INTRODUCTION

The nowadays industrial rotor machines are more flexible and often operating with ultra-high speed. Therefore, the suspension systems must to advanced and high reliable. Another problem is connected with power consumptions, the modern suspensions should be low-power systems.

Active magnetic bearings have many disadvantages connected with complicated control hardware, such as expensive digital processors, amplifiers with limited bandwidth, sensitive sensors, and software. Thus, these systems are itself low reliable and have high energy loss index.

Passive magnetic bearings do not require control and measure hardware and advanced software, thereby they have the potential to increase system efficiency and reliability. Another advantage of PMBs is positive stiffness and self-stability. What more, they can operate with larger rotor-stator gaps since the levitation force for active magnetic bearings is inversely proportional to the square of the rotor-stator gap. The disadvantage of PMBs is lack of stiffness control due to e.g. rotor displacements and lower damping than similar size active magnetic bearings.

The beginning of the development of magnetic bearing combined with the first patent of American scientist Jesse Beams from University of Virginia during the Second World War (Beams, 1964). Passive magnetic levitation receiving one degree of freedom by using permanent magnets was achieved and described by Jansen and Di Russo (1996), Ohji et al. (1999) and Fremerey (2000). The use of superconductors in the art of passive magnetic bearings was described by Hull and Turner (2000) and Hull et al. (1994). Several papers were also published on research of the coefficients of stiffness and damping of passive magnetic bearings. Their creators are Satoh (1996), Ohji (1999) as well as previously mentioned Jansen and Di Russo (1996).

This paper concerns the design, implementation, and research studies of the PMB which consists of the permanent magnets based on the Halbach-array configuration. The main objective of this study was to design and execution of the analytical model, experimental tests and model verification of the passive magnetic bearing based on permanent magnets (Fig. 1). For this purpose the PMB test rig was designed and constructed. The experimental characteristics of the magnetic force due to radial rotor displacement were measured in the passive bearing plane and compared with the analytical one.

1.1. Halbach arrays

Using the passive magnetic bearings in certain applications, we need to take into account the occurrence of radial component in the case of axial bearings and axial component in the case of radial bearings. Journal bearings, in addition to passing load forces of the rotor, rotor weight and damping must take into account the existence and impact of this negative component forces. Therefore, in the design of passive bearings Halbach-arrays are introduced. Halbach-array is a special setup and configuration of permanent magnets, so that you can get the concentration of magnetic flux in a specific, desired items, and remove it from less important or unwanted places (Halbach, 1980).

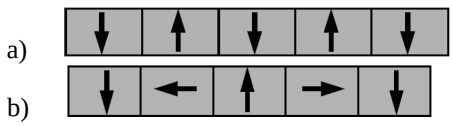

Fig. 1. Sample Halbach-array configurations, a) 180° and b) 90°

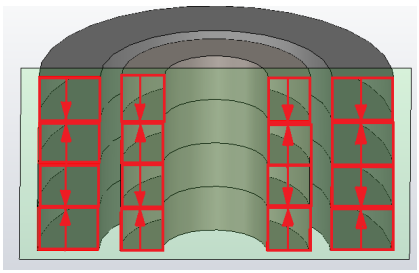

Fig. 2. Cross-section of the PMB with Halbach-array configuration

Among the Halbach arrays, to guide the magnetic field in the desired way, we can distinguish boards between 180° and 90°. These terms relate to the relationship between the magnetization vectors.

In the construction of the passive radial magnetic bearing 180° Halbach-array was used. This kind of magnetic bearings belongs to the repulsive magnetic bearings. Full configuration of constructed Halbach-array is presented in Fig. 2.

2. DESCRIPTION OF DESIGNED RIG

The examined passive magnetic bearing is composed of four pairs of the Neodymium-iron-boron (NdFeB) magnets rings. These rings are axially magnetized, which means that magnetic poles are placed on the flat circle sides of the magnets (see Fig. 2). The dimensions of the magnets are shown in Tab. 1.

Tab. 1. Magnets dimensions

	Material	Outer diameter\ D_Z [mm]	Inner diameter D_w [mm]	Thickness g [mm]
Outer ring	NdFeB N38	75	49	10
Inner ring	NdFeB N38	40	22	10

Magnetic parameters of the magnets are grouped in Tab. 2.

Tab. 2. Magnetic parameters of magnets

Parameter	Symbol	Unit	Value	
			MP1	MP2
Material	-	-	N38	N38
Remnant flux density	B_r	[T]	1.25	1.1
Coercivity	H_c	[kA/m]	899	854
Magnetic energy	$(BH)_{max}$	[kJ/m^3]	302	243
Temp. of work	T_c	[°C]	120	180
Magnetic flux	$\phi_{e.max}$	[mWb]	4670e-3	4890e-3

The base of the magnetic bearing stator is made of a aluminum alloy PA11 and PA6, which are nonmagnetic materials. Stator consists of five parts, namely: the vertical bracket left and right (Fig. 3 {2}), middle base (Fig. 3, {3}) and the hub mounting magnets (Fig. 3, {1}). Additionally, on the stator is mounted the handle of distance sensors made of aluminum (Fig. 3, {4}).

The rotor shaft was made of constructional steel (Fig. 4, {1}) but the post of inner magnets (Fig. 4, {3}) is made of brass (Fig. 4, {4}). Distance ring (Fig. 4, {7}) are made of brass also and is mounted with a steel nut (Fig. 4, {2}). On the rotor a steel blade to implicate unbalance the rotor is placed (Fig. 4, {6}). To reduce the air gap between inner and outer magnets in magnetic bearing, the sleeve was used made of soft magnetic material (Fig. 4, {5}).

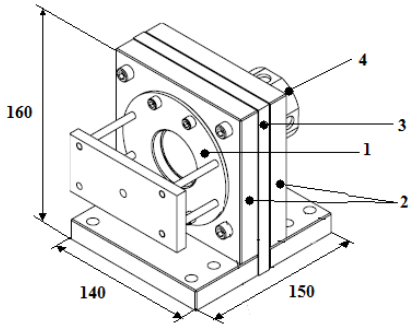

Fig. 3. Stator of the passive magnetic bearing

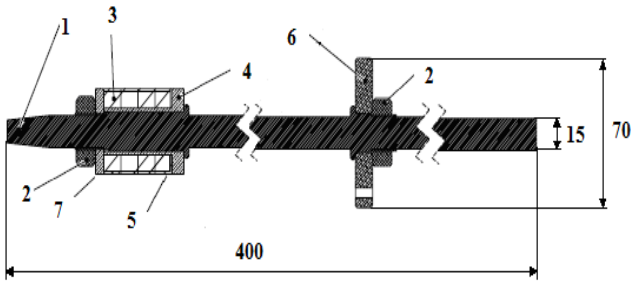

Fig. 4. Cross-section of rotor with passive magnetic bearing

3. SIMULATION RESULTS

To analyze the magnetic bearings and to estimate their radial force distribution, 3D models of the passive magnetic bearing were built. Simulation calculations were made by using the FEM via Comsol Multiphysics ver. 3.5a software. The magnetostatic module of Comsol environment was used to analyze the magnetic field distribution of the passive magnetic bearings with Halbach-array.

3.1. FEM magnets model definition

Analysis of the magnetic field of magnetic bearing is a magnetostatic problem with no current. This problem we can solve using a scalar magnetic potential. In regions with no current, where:

$$\nabla \times H = 0 \tag{1}$$

where: H – magnetic field, ∇ – nabla operator.

We can define the scalar magnetic potential V_m, from the following relation:

$$H = -\nabla V_m \tag{2}$$

It is analogous to the definition of the electric potential for static electric field.

Using the major relation between the magnetic flux density and magnetic field, which is described by:

$$B = \mu_0 (H + M) \tag{3}$$

where: B – magnetic flux density, M – magnetization vector.

Together with equation:

$$\nabla \times B = 0 \tag{4}$$

We can simply derive an equation for V_m,

$$-\nabla(\mu_0 \nabla V_m - \mu_0 M_0) = 0 \tag{5}$$

Equation (3) supplemented by the following expressions:
– first Maxwell equation for current-less area:

$$\mu_0 rotH = 0 \tag{6}$$

– or first Maxwell equation for conducive area:

$$rotH = J \tag{7}$$

where: J – current density,
– magnetic field source-less condition:

$$divB = 0 \tag{8}$$

These equations are true for stationary magnetic field of the permanent magnet in an environment of soft ferromagnetic. In order to design model of magnetic field of passive magnetic bearing, the above conditions should be applied. The analytical model of magnetic phenomena will be developed by using Comsol Multiphysics, and 3D discrete model of the PMB will be presented.

3.2. Boundary conditions

Along the boundaries far away from the two pairs of magnets (Fig. 5), the magnetic field should be tangential to the boundary as the flow lines should form closed-loops around the modeled magnets. The natural boundary condition is expressed by:

$$n\left(\mu_0 \nabla V_m - \mu_0 M_0\right) = nB = 0 \tag{9}$$

where: n – boundary normal pointing out from the inner magnet rings.

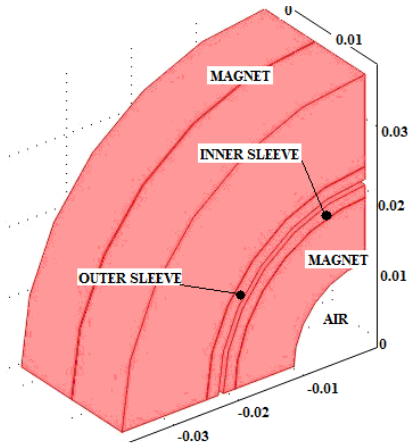

Fig. 5. Finite element model - magnets geometry

Therefore the magnetic field is made tangential to the boundary by a Von Neumann condition on the magnetic potential. Along the symmetry boundary below the magnet, the magnetic field should be tangential, and thus we can apply the same Von Neumann condition there.

Against, the magnetic field should be normal to the symmetry boundary, which is located at the front of the magnet rings cross-plane (see Fig. 5). Thus, the magnetic flow lines have formed of the closed-loops rings around the magnet. This means that the magnetic field is symmetric with respect to the boundary. This can be achieved by setting the potential to zero along the boundary, and thus making the potential anti-symmetric with respect to the boundary.

3.3. Subdomain settings

The Fig. 5 shows all highlighted subdomains in magnetic bearing finite element model. These are: magnets of stator, magnets of rotor, outer sleeve, inner sleeve and ambient air. In order to get the detailed finite element model of the PMB, the proper parameters need to by find in the right domain of the geometric model.

Selected following settings and parameters of the highlighted domains in the magnetic bearing model are presented in Tab. 3.

Tab. 3. Subdomain settings

Settings	Subdomain 1,2	Subdomain 3	Subdomain4
Description	Rotor Magnet, Stator Magnet	Magnetically Soft Sleeve	Air
Constitutive relation	$B = \mu_0 H + \mu_0 M$	$B = \mu_0 \mu_r H$	$B = \mu_0 \mu_r H$
μ_r	-	6980	1

3.4. FEM calculations

Next, the PMB mesh model is developed. Setting the relevant parameters the mesh model is extremely important to correctly estimate all properties of the magnetic bearings and determine the maximum radial force of the bearing. Mesh was concentrated in the most important places of the magnetic bearing model, which are air gaps between pairs of stator and rotor magnets. As the most optimal mesh element tetrahedron was used. The maximum size of the mesh element was defined as 5-7% of the smallest dimension of the geometric domain. Maximum element size scaling factor was chosen as 0.5. Mesh curvature factor was set as 0.25. In the magnetic bearing air gaps, inner and outer sleeves, the gap element was used. Gap element is the special kind of mesh element. It is particularly important whenever a big impact on the field distribution have air gaps in model. Gap element reduces the growth of algebraic matrix equations in the calculations. To reduce the size of the field surrounding the magnet rings model, the infinite element was used, which improves the results of calculations by a few percent and reduced the number of elements in finite element model.

The magnetostatic solver was used to calculate the radial force and predict the distribution of magnetic field in the PMB with Halbach-array. The 3D magnetic bearing mesh model is illustrated in Fig. 6. The model have 1282681 elements. To compute magnetic forces and torques in the AC/DC Comsol Module, four methods are available. The most general method is to use the Maxwell Stress tensor described below. Force and torque calculations using Maxwell's stress tensor are available in the application modes for electrostatics, magnetostatics, and quasi-statics. In case of the magnetostatics and quasi-statics the Maxwell Stress tensor

is given by:

$$n_1 T_2 = -\frac{1}{2} n_1 (H \cdot B + n_1 \cdot H) B^T \qquad (10)$$

where: n_1 – outward normal from the object.

The Maxwell stress tensor was integrated over the inner magnets surface.

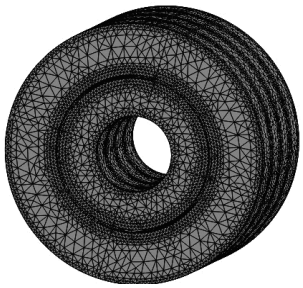

Fig. 6. 3D mesh model of passive magnetic bearing

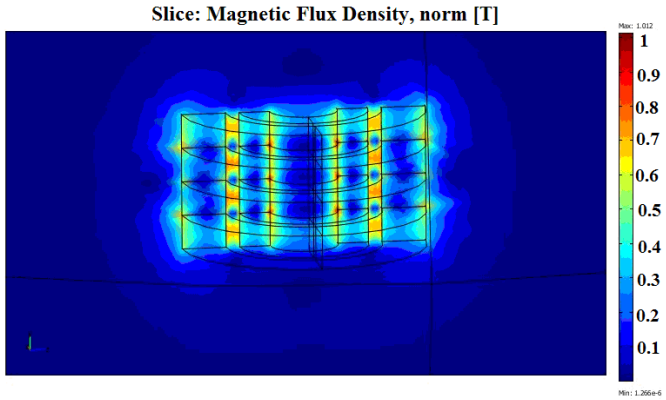

Fig. 7. Magnetic flux density in cross section of magnetic bearing

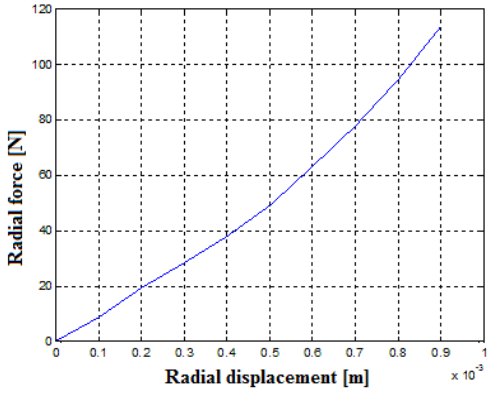

Fig. 8. Displacement stiffness characteristic of the PMB

Three-dimensional model of magnetic bearings was used to compute the magnetic potential, magnetic flux density and magnetic energy in the air gap.

In Fig. 7 we could observed places in air gap where the field reaches the highest values and where it falls significantly. This is caused by build Halbach-array. The gaps in magnetic field observe in Fig. 7 are typical for this kind of Halbach-arrays.

Depending on the movement of the rotor in the magnetic bearing plane, the air gap is changed, and therefore the repulsive force of the magnets changed too. For the different positions of the rotor in the bearing plane, the power calculations were made based on a reduced finite element model of the PMB. The results obtained are summarized and presented in the form of static characteristics (Fig. 8).

4. EXPERIMENTAL TESTS

The experimental study have allowed to verify the finite element model of the PMB and to analyze the design and assessment of its fairness and accuracy of design assumptions bench. The lab test rig is presented in Fig. 9. The lab stand consists of rotor with electrical drive and elastic clutch, the rotor is supported by one ball bearing and passive magnetic bearing located at the end of the rotor. In order to measure the magnetic radial force, the tensometer force sensor was assembled. The radial displacement of the rotor was measured in two directions *x*-*y* by using inductive sensors. The total weight of the rotor is 1.07 kg, and total length of 0.4 m. The nominal radial air gap is equal to 0.001 m. The actual physical model has become a reference for early design and simulation tests.

Fig. 9. Test rig

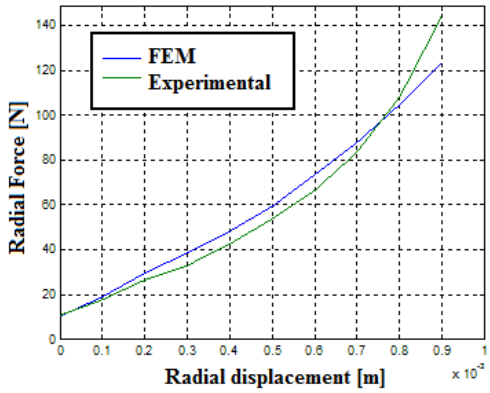

Fig. 10. Measured and calculated PMB stiffness

The first stage of the experimental tests were static stiffness measurements with no rotating rotor. As a result, the values of the magnetic repulsive forces in the radial direction due to change of the air gap were determined. Depending on the rotor load, measured by electronic scales, the value of its shipments and dial indicator has been observed using inductive sensor.

Next, the measured radial magnetic bearing force due to rotor displacements in the range of the air gap was compared with the FEM calculations (see Fig. 10).

Fig. 10 shows the rotor displacement as a function of radial load for the experimental data and finite element model. The slopes (stiffness) of these curves match quite well and equals $1.28 \cdot 10^5$ N/m. The finite element model of the PMB is sufficiently consistent with the laboratory model. Thus, the finite element method, with appropriate choice of parameters, a careful analysis and accurate modeling, may be used with quite good results in the design of passive bearings and to assess the pre-load magnetic bearing.

The axial stiffness of the passive magnetic bearing is more stronger than in radial direction and is not presented in this paper.

5. SUMMARY

A completely passive magnetic bearing rig was designed, constructed, and tested in this work. The experimental and simulation results are well matched, thus the finite element methods can be used to accurately design the size and number of the magnets for the radial support of the bearings.

The implementation of the passive magnetic bearing requires a careful analysis of the magnetic field generated by permanent magnets and assesses their material aspects. Obtained and desired distribution of magnetic field strength determines the values of the bearings, radial and axial component. The introduction of the Halbach-arrays allows the adequate orientation of the magnetic field in the placenta, and to reduce the negative impact of the active component forces. The use of Halbach-arrays and a thorough assessment and analysis of magnetic bearings, allow to develop and to implement the high performance passive magnetic bearings. Submission of the magnets in different directions of polarization is a very difficult task and unfortunately expensive too, thus always some assumption should be taken into account.

REFERENCES

1. **Asami K.. Chiba A., Rahman M. A., Hoshino T. A. H. T., Nakajima A. A. N. A**. (2005),Stiffness analysis of a magnetically suspended bearingless motor with permanent magnet passive positioning, *IEEE Transactions on Magnetics*, Vol. 41, 3820-3822.
2. **Beams J.** (1964), Magnetic Bearings, Paper 810A, *Automotive Engineering Conference*, Detroit, Michigan, USA, SAE.
3. **Bolkowski S., Stabrowski M., Skoczylas J., Sroka J., Sikora J., Wincenciak S.** (1993), *Komputerowe metody analizy pola elektromagnetycznego*, WNT, Warszawa.
4. **Burcan J.** (1996), *Łożyska wspomagane polem magnetycznym*, WNT, Warszawa.
5. **Delmare J., Rulliere E., Yonnet J. P.** (1992), Classification and Synthesis of Permanent Magnet Bearing Configurations, *IEEE Transactions on Magnetics*, Vol. 31, No. 6, 4190-4192.
6. **Earnshaw S.** (1848), On the Nature of the Molecular Forces which regulate the Constitution of the Luminiferous Ether, *Transactions of the Cambridge Philosophical Society*, Vol. VII, Part I, 97-112, London.
7. **Filatov A., Maslen E. H.** (2002), A method of non-contact suspension of rotating bodies using electromagnetic forces, *Journal of Applied Physics*, Vol. 91, No 4.
8. **Fremerey J. K.** (1999), *Magnetlager*, DE199 44 863 A1.
9. **Fremerey, J. K.** (2000), A 500-Wh Power Flywheel on Permanent Magnet Bearings, *Fifth International Symposium on Magnetic Suspension Technology*, 287–295.
10. **Geim A. K., Simon M. D., Boamfa M. I., Heflinger L. O.** (1999), Magnetic Levitation at Your Fingertips, *Nature*, Vol. 400, 232–324.
11. **Gosiewski Z., Falkowski K.** (2003), *Wielofunkcyjne łożyska magnetyczne*, Biblioteka Naukowa Instytutu Lotnictwa, Warszawa.
12. **Gosiewski Z., Osiecki W., Panasiuk M.** (2007), *Elementy mechatroniki*, Wydawnictwa WAT, Warszawa.
13. **Halbach K.** (1980), Design of permanent multipole magnets with oriented rare earth cobalt material, *Nucl. Instr. Meth.*, Vol. 169, 1-10.
14. **Hull J. R., Mulcahy T. M., Uherka K. L., Erck R. A., Abboud R. G.** (1994), Flywheel Energy Storage Using Superconducting Magnetic Bearings, *Appl. Supercond.*, Vol. 2, 449–455.
15. **Hull J. R., Turner L. R.** (2000), Magnetomechanics of Internal-Dipole, Halbach-Array Motor/Generators, *IEEE Transactions on Magnetics*, Vol. 36, No. 4, 2004–2011.
16. **Jansen R., DiRusso E.** (1996), *Passive Magnetic Bearing with Ferrofluid Stabilization*, NASA TM–107154.
17. **Ohji T., Mukhopadhyay S. C., Iwahara and Yamada S.** (1999), Permanent Magnet Bearings for Horizontal- and Vertical-Shaft Machines: A Comparative Study, *Journal of Applied Physics*, Vol. 31, 8, 4648–4650.
18. **Post R. F., Ryutov D. D.** (1997), *Ambient-Temperature Passive Magnetic Bearings: Theory and Design Equations*, LLNL Pub. #232382.
19. **Siebert M, Ebihara B., Jansen R**. (2002), *A Passive Magnetic Bearing Flywheel*, NASA/TM—2002-211159, IECEC2001 –AT–89.
20. **Yonnet J. P.** (1981), Permanent Magnet Bearings and Couplings, *IEEE Transactions on Magnetics*, Vol. Mag-17, No. 1, 1169-1173.